

The multiple spectroscopic and photometric periods of DI Cru \equiv WR 46 ¹

Alexandre S. Oliveira², J. E. Steiner² and M. P. Diaz²

alex@astro.iag.usp.br, steiner@astro.iag.usp.br, marcos@astro.iag.usp.br

ABSTRACT

In an effort to determine the orbital period of the enigmatic star DI Cru \equiv WR 46 \equiv HD 104994, we made photometric and spectroscopic observations of this object between 1996 and 2002. Both photometric and spectroscopic characteristics are quite complex. The star is highly variable on short (few hours) as well as on long (few months) time-scales.

The optical spectrum is rich in strong emission lines of high ionization species such as He II, N IV, N V and O VI. Weak emission of C III and H β is also present. Emission lines have been compiled and identified from the ultraviolet to the infrared. In the UV, emission of O V and N IV is also observed, together with very weak emission of C IV. The N V 4603+19Å/He II 4686Å line ratios vary by a significant amount from night to night. Temporal Variance Spectrum – TVS – analysis shows that the He II 4686Å line has P Cyg-like variable absorption, while N V 4603/19Å lines have a strong and broad variable component due to the continuum fluorescence from a source (stellar atmosphere/optically thick wind) of variable temperature. We also show that the object has variable degree of ionization, probably caused by wind density variation.

The star presents multiple periods in radial velocity and photometry. We derived, from our data, a main radial velocity period of 0.3319 d with an amplitude of $K = 58 \text{ km s}^{-1}$. This period is similar to the value found by Marchenko et al. (2000). When at intermediate brightness level, this period is also seen in the photometric measurements. When the star is at bright phase, the photometric variations do not present the same period. Photometric periods ranging from 0.154 to 0.378 d are present, consistent with observations reported by other authors. Besides the 0.3319 d period other spectroscopic periods are also seen. On distinct epochs, the periods are different; Marchenko et al. (2000) interpreted the 0.3319 d period as the orbital one. Although we do not discard this possibility, the true binary nature (e.g. long term coherence or detection of a secondary star) has not yet been demonstrated.

DI Cru is a Population I WR object. Given the similarities (e.g. multiple periods likely due to non-radial oscillations), it could be interpreted as a luminous counterpart of the qWR star HD 45166.

Subject headings: stars: individual (DI Cru) — stars: Wolf-Rayet — stars: peculiar — binaries: spectroscopic — stars: oscillations

²Instituto de Astronomia, Geofísica e Ciências Atmosféricas, Universidade de São Paulo, CP 9638, 01065-970 São Paulo, Brazil

¹Based on observations made at Observatório do Pico dos Dias/LNA, Brazil, and at the 1.5m ESO telescope at La Silla, Chile.

1. Introduction

DI Cru \equiv WR 46 \equiv HD 104994 is a Wolf Rayet star that has been classified as a peculiar early WN, weak lined object. In The VIIth Catalogue of Galactic Wolf-Rayet Stars (van der Hucht 2001) it was classified as WN3 pec, where the "pec" suffix indicates the presence of strong O VI 3811/34Å

emission lines. There are only three WR stars of the nitrogen sequence in this catalog that display strong O VI emission lines. The other stars are WR 109 (also known as V617 Sgr (Steiner et al. 1999) and WR 48c, also known as WX Cen (Diaz and Steiner 1995). Both of them have well defined short orbital periods. WR 156 is also reported in the Catalog as having O VI emission lines. However, the N V 4945Å line is not present in the spectrum published by Marchenko et al. (1998a) and O VI lines are not visible in the spectrum published by Hamann et al. (1995). DI Cru was classified by Smith et al. (1996) – SSM96 – in their three-dimensional classification system as WN3b pec. The letter "b" stands for $\text{FWHM}(\text{He II } 4686\text{Å}) > 30 \text{ Å}$ or 1920 km s^{-1} .

The Einstein Observatory IPC detected DI Cru as a source with a derived X-ray luminosity $L_X(0.2 - 4 \text{ KeV}) \sim 3 \times 10^{33} \text{ erg s}^{-1}$ with an estimated distance of 8.7 kpc (Pollock 1987). It was also detected by the ROSAT PSPC instrument (Wessolowski et al. 1995). van der Hucht et al. (1988) list a distance of 3.44 kpc and an absolute magnitude of $M_V = -2.8$. In their analysis of Wolf-Rayet stars distribution in the Galaxy, on the basis of their distance determination by spectroscopic parallaxes, Conti and Vacca (1990) estimated a distance of 6.3 kpc, assuming $M_V = -3.8$ and $(b - v)_0 = -0.20$. These values were derived under the hypothesis that the star has standard WN3 properties. Veen and Wieringa (2000) derived a lower limit of 1.0 kpc based on the upper limits to the radio fluxes at 3 and 6 cm and on an adopted mass-loss rate of $\log \dot{M} (M_\odot \text{ yr}^{-1}) = -5.2$. In addition to this, Tovmassian et al. (1996) place the system in an OB association with 11 other stars at a distance of 4.0 kpc.

Monderen et al. (1988) found photometric variability with 0.075 mag amplitude in the V filter and time-scale of about 0.125 d. In a follow-up photometric study, van Genderen et al. (1991) suggest a binary nature with an orbital period of 0.2824 d and an asymmetric 0.15 mag amplitude light curve. These authors also suggest that the emission lines are emitted by a circumstellar envelope.

Crowther et al. (1995) - CSH95 - presented ultraviolet and optical observations of DI Cru and made a detailed wind model analysis of this ob-

ject in the context of weak-lined WNE stars. They concluded that the star is well modeled as a population I object with strong wind. They also concluded, however, that its location in the HR diagram and its CNO abundances are quite anomalous and are not predicted by theoretical model evolution for WR stars. These authors found that oxygen is overabundant by a factor of 2 ($\text{O/N} \sim 0.1$) and that the upper limit for carbon is $\text{C/O} < 0.3$. An independent determination of the distance to the star on the basis of the galactic rotation curve was also made by these authors, who found a distance $d = 4.0 \pm 1.5 \text{ kpc}$. The derived luminosity is $\log L/L_\odot = 5.53$, the mass, $M = 14 \pm 1 M_\odot$ and $\log \dot{M}/M_\odot \text{ yr}^{-1} = -5.20$.

A preliminary radial velocity curve of the emission lines of DI Cru was published by Veen et al. (1995) and showed an amplitude of about 100 km s^{-1} with the 0.28 d period. The binary nature of the system seemed to be confirmed. However, from analysis of the radial velocity of the N V 4603/19Å and the He II 4686Å lines, Niemela et al. (1995) determined a period of 0.311274 d, quite distinct from the 0.28 d period found before. These authors suggest DI Cru to be an evolved binary system containing an accretion disc. Based on polarimetric observations they estimate a distance of about 2 kpc and an absolute magnitude of $M_V = -1.6$. van Genderen et al. (1991) and also Veen et al. (1995) proposed that the star is a binary system in which the low mass object is a white dwarf – a configuration difficult to explain considering the theory of binary evolution.

Marchenko et al. (1998b) reported the discovery, using the Hipparcos satellite, of long term photometric variations with approximately 0.2 mag amplitude (V_j). Long term variations in the equivalent width of the He II 5411Å emission line correlated with these photometric variations were also reported (Veen et al. 1999). Marchenko et al. (2000) - Mar00 - presented extensive spectroscopic and photometric monitoring of DI Cru and showed that the star reveals periodic variations with a period of $0.329 \pm 0.013 \text{ d}$. Although these authors interpret the system as a classical population I WR star in a binary system, they found that the radial velocity modulation disappears from time to time, establishing a new puzzle.

Recently, Veen et al. (2002a,b,c) – Vee02a,b,c – in a series of papers, made a detailed analy-

sis of photometric and spectroscopic data. They found that the star has presented distinct periods and interpreted this as evidence for either multiple non-radial pulsation periods or gradual change of the underlying clock rate. They discussed a variety of scenarios to explain the set of observations and ruled out the model of single star rotation as the main cause of photometric and spectroscopic variability. Between the two remaining possibilities – non-radial pulsation or binary signature – they favored the former one but concluded that the enigma of DI Cru has not yet been solved, leaving room for further investigation.

Steiner and Diaz (1998) included this star in a group of 4 objects they called the V Sagittae stars. This group of objects is composed of galactic binary stars that share many photometric and spectroscopic observational properties that are not found among the canonical cataclysmic variables or WR stars. The stars of this class are spectroscopically characterized by the simultaneous presence of emission lines of O VI and N V and by the strength of the He II 4686Å emission line relative to H β usually larger than 2. There is also indication of strong wind in all the systems, as can be concluded from the clear P Cygni profiles, seen in all objects (see also Steiner et al. (1999) and Diaz (1999)). He I lines are very weak or most frequently absent. No evidence of atmospheric absorption features from the secondary star has been published so far. The other three members of this group are: V Sge (Herbig et al. 1965), V617 Sgr = WR 109 (Steiner et al. 1999; Cieslinski et al. 1999) and WX Cen = WR 48c (Diaz and Steiner 1995). The orbital periods of these stars are 12 hr, 5 hr and 10 hr, respectively. One possible interpretation of these stars is that they are the galactic counterpart of the Close Binary Supersoft X-ray Sources (CBSS) seen in the Magellanic Clouds and in M31 (Steiner and Diaz 1998). The most popular model to explain the properties of the CBSS is that of hydrostatic nuclear burning on the surface of a white dwarf (van den Heuvel et al. 1992). This stable nuclear burning can occur when the mass transfer ratio is very high ($10^{-7} M_{\odot} yr^{-1}$), a situation that occurs in systems with mass ratios inverted ($q = M_2/M_1 < 1$) when compared to those usually found in cataclysmic variables (Kahabka and van den Heuvel 1997).

The suggestion that DI Cru is a V Sagittae star

has been criticized by Mar00 and by Vee02a,b. Their main arguments are: a) unlike CBSS/V Sge stars, DI Cru has a strong wind and b) the population I model calculated by Crowther et al. (1995) describes well the line profiles, and the derived properties are similar to other weak lined WNE stars. As we will show in Section 6.3, we argue that DI Cru is a population I WR and not a V Sge star. However, the first of the two arguments above is not correct since both classes present strong wind. It is curious that these two groups of objects are members of completely distinct stellar paradigms and, yet, present similar spectral properties. WR stars are post main sequence phases of very massive ($\sim 60 M_{\odot}$) stars – a young population. Currently they are in central helium (N sequence) or carbon (C sequence) burning phases. In contrast, V Sge stars are an evolutionary phase of a binary system containing a white dwarf – an intermediate mass, old population star.

In the present work we show the results of the analysis of photometric and spectroscopic data on DI Cru obtained during the years 1996 – 2002. In Section 2 we describe the observations and data reduction procedures, while the optical spectrum is presented and discussed in Section 3. Sections 4 and 5 present the search for periodicities in this system, while Sections 6 and 7 present general discussions and the conclusions.

2. Observations and data reduction

2.1. Photometric observations

The photometric data on DI Cru were obtained between 1996 and 1999, in a total of 45 nights, using the 60 cm Boller & Chivens telescope of the University of São Paulo and the 60 cm Zeiss-Jena telescope, both at the Laboratório Nacional de Astrofísica in Itajubá, Brazil. In these 4 years, 4 different CCDs were used to carry out the observations. The images were obtained through the Johnson V band or in white light and cover fields between 2.7' x 3.6' and 7.9' x 11.9', which contain DI Cru and the same four comparison stars always used in the differential photometry.

Table 1 gives the journal of photometric observations. Bias and flatfield images were obtained to correct for undesirable instrumental signatures. Most of the images present an overscan region used for correction offsets in the mean bias level.

The data reduction was performed in the standard way, using the IRAF² routines. Differential aperture photometry was executed using the DAOPHOT II routines package. We applied, to these data, period search routines based on Fourier analysis with cleaning of spectral windows effects (CLEAN) (Roberts et al. 1987), Phase Dispersion Minimization method (Stellingwerf 1978) and also Lomb-Scargle method (Scargle 1982).

2.2. Spectroscopic observations

The spectroscopic observations were carried out with the 1.6 m telescope and the Boller & Chivens Cassegrain and Coudé spectrographs. At the Cassegrain spectrograph, we used a 1200 l/mm dispersion grating to obtain 3 spectra with $\sim 2\text{\AA}$ resolution (FWHM). A total of 124 Coudé spectra were obtained with the 600 l/mm and 1800 l/mm gratings, resulting in $\sim 0.7\text{\AA}$ and $\sim 0.2\text{\AA}$ FWHM resolution, respectively. Table 2 presents the journal of spectroscopic observations. We obtained several bias and dome flatfield exposures to correct for the readout pattern and sensitivity variations on the detectors. Dark current correction was not necessary. The slit width was sized to the seeing conditions at the time of observation. We took exposures of calibration lamps between each star exposure to obtain the pixel-wavelength transformation. The solutions obtained were interpolated to the individual star exposures. The image reductions, spectra extraction and wavelength calibration were attained with IRAF standard routines.

An additional spectroscopic observational mission was made with the FEROS – Fiber-fed Extended Bench Optical Spectrograph – (Kaufer et al. 1999) at the 1.52 m telescope of ESO (European Southern Observatory) in La Silla, Chile. The FEROS spectrograph uses a bench mounted Echelle grating with reception fibers in the Cassegrain focus. It supplies a resolution of $R = 48000$, corresponding to 2.2 pixels of 15 micrometers, and spectral coverage from 3600 \AA to 9200 \AA . A completely automatic online reduction system is available and was adopted by us. Readout time was approximately 7 minutes.

²IRAF is distributed by the National Optical Astronomy Observatories, which are operated by the Association of Universities for Research in Astronomy, Inc., under cooperative agreement with the National Science Foundation.

3. The optical spectrum

3.1. Line identification

The FEROS spectrum, with its high resolution and wide spectral coverage from 3800 \AA to 8800 \AA , gives us the opportunity to identify the emission as well as the absorption features with high accuracy over a wide spectral range. The spectrum of DI Cru is quite rich in emission lines, mostly from high ionization species such as He II, N IV, N V and O VI (see Table 3).

Figures 1, 2 and 3 show our spectra obtained at LNA. These figures illustrate quite well the fact that the O VI 3811/34 \AA and N V 4945 \AA are much narrower than He II 4686 \AA , while N V 4603 \AA has a narrow and a broad component.

We have compiled the CNO emission lines from the literature and organized them in a table with similar configurations, term by term (see Table 4). From this table it is clear that the spectrum is dominated by only three high ionization species: He II, N V and O VI. The only O V – N IV – C III lines that have been observed are the terms ($2p\ ^1P^0 - 2p^2\ ^1D$) and ($3s\ ^3S - 3p\ ^3P^0$).

We used Coudé spectra centered at 8300 \AA to search for spectroscopic evidence of a possible secondary star. These spectra were divided by the spectra of hot calibration stars to eliminate the atmospheric absorption lines. We also obtained spectra of cool comparison stars (of M, G and K spectral types) with the same instrumental configuration and did the same process in order to compare the characteristic spectral lines of the cool stars to the lines of DI Cru. We could not see any evidence of a cool component. In our high-resolution FEROS spectra we were also unable to detect any spectral feature of a hypothetical secondary star.

The terminal wind velocity, as estimated from He II emission lines, is $v^*(\text{HWZI}) = 2200\text{ km s}^{-1}$.

3.2. Line variability

The line profile and intensity variability has been extensively discussed by Mar00 and by Vee02b. Line fluxes vary from long time-scales, correlated with the overall photometric variability, to time-scales as short as minutes, with flares in the He II lines.

The ratio between the N V 4603/19 \AA and He II

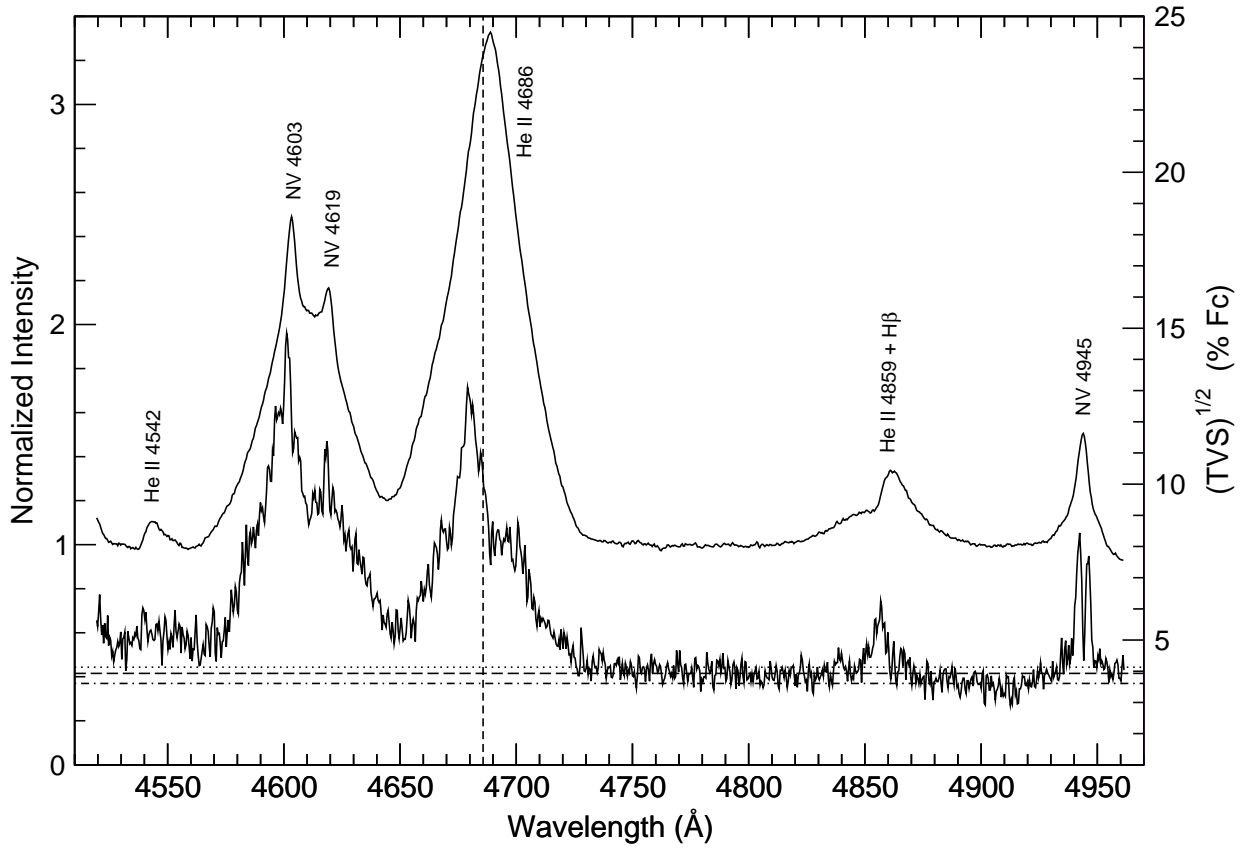


Fig. 1.— Average Coudé spectrum (above) and TVS (below) calculated from the LNA data, both centered at 4750Å. The vertical dashed line represents the He II 4686Å rest wavelength. The TVS statistical threshold significance for $p=1\%$, 5% and 30% are represented by the dotted, dashed and dot-dashed horizontal lines, respectively.

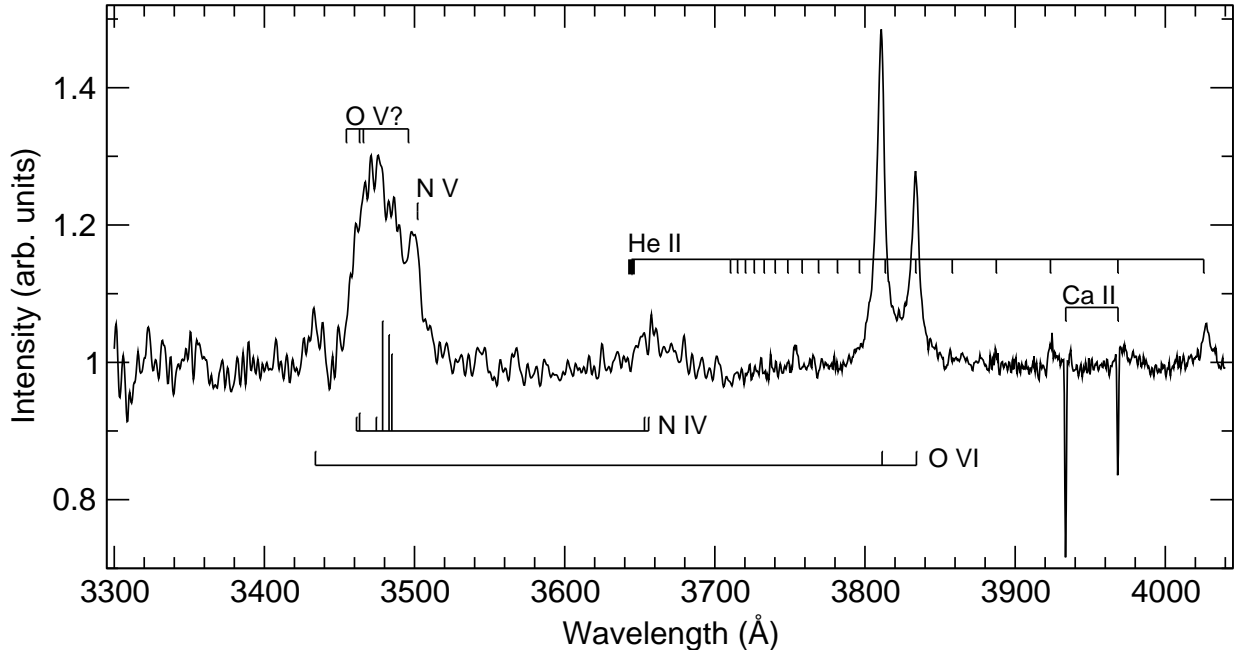


Fig. 2.— The average blue spectrum of DI Cru.

4686Å seems to be quite variable, showing significant variations from night to night. This variability is well illustrated by comparing the spectrum from 1999 April 1, (Figure 3) with the average spectrum shown in Figure 1. On 1999 April 1 the N V 4603/19Å was unusually strong, being more intense than He II 4686Å. A significant variability in the N V to He II line ratio was also noticed by Vee02b.

In order to study the line variability in a more objective way, we computed the Temporal Variance Spectrum (TVS). In this procedure the temporal variance is calculated for each wavelength pixel from the residuals of the continuum normalized spectra. In our TVS analysis we calculate the square root of the variance as a function of wavelength. For further details and discussion of this method, see Fullerton et al. (1996). The TVS of our medium resolution LNA spectra (81 spectra obtained on 1998 April 10, 11 and 12) is shown in Figure 1. The first thing to notice is the striking difference between the TVS profile of the N V 4945Å (narrow) line and the (broad) lines of He II and N V 4603/19Å. This illustrates well the two regimes described in Fullerton et al. (1996): the two peaked profile resulting from a radial velocity

variation and a true line profile variation – lpv . When the line has no intrinsic variation but is displaced by radial velocity only, it introduces a double peak profile as illustrated in Figure 1 of Fullerton et al. (1996). In this case one expects $\sigma/I \sim K/\text{FWHM}$. In the case of N V 4603Å and of He II 4686Å, the TVS profile is much more similar to a true line profile variation, where the TVS profile is filled and the two peaks disappear.

Another remarkable characteristic is the difference in σ/I for the He II 4686Å ($\sigma/I \sim 5\%$) and N V 4603Å ($\sigma/I \sim 10\%$). This indicates that the observed profile of N V 4603Å varies more than He II 4686Å (by about a factor of two).

Finally, the He II 4686Å shows a σ/I ratio that depends on the velocity along the profile. While the line profile has a maximum red-shifted by $\Delta v = +175 \text{ km s}^{-1}$, the TVS has its maximum at negative velocity ($\Delta v = -350 \text{ km s}^{-1}$). We tentatively explain this effect in terms of a variable P Cyg absorption, causing both the displacement of the emission peak to the red and maximum variance in the blue.

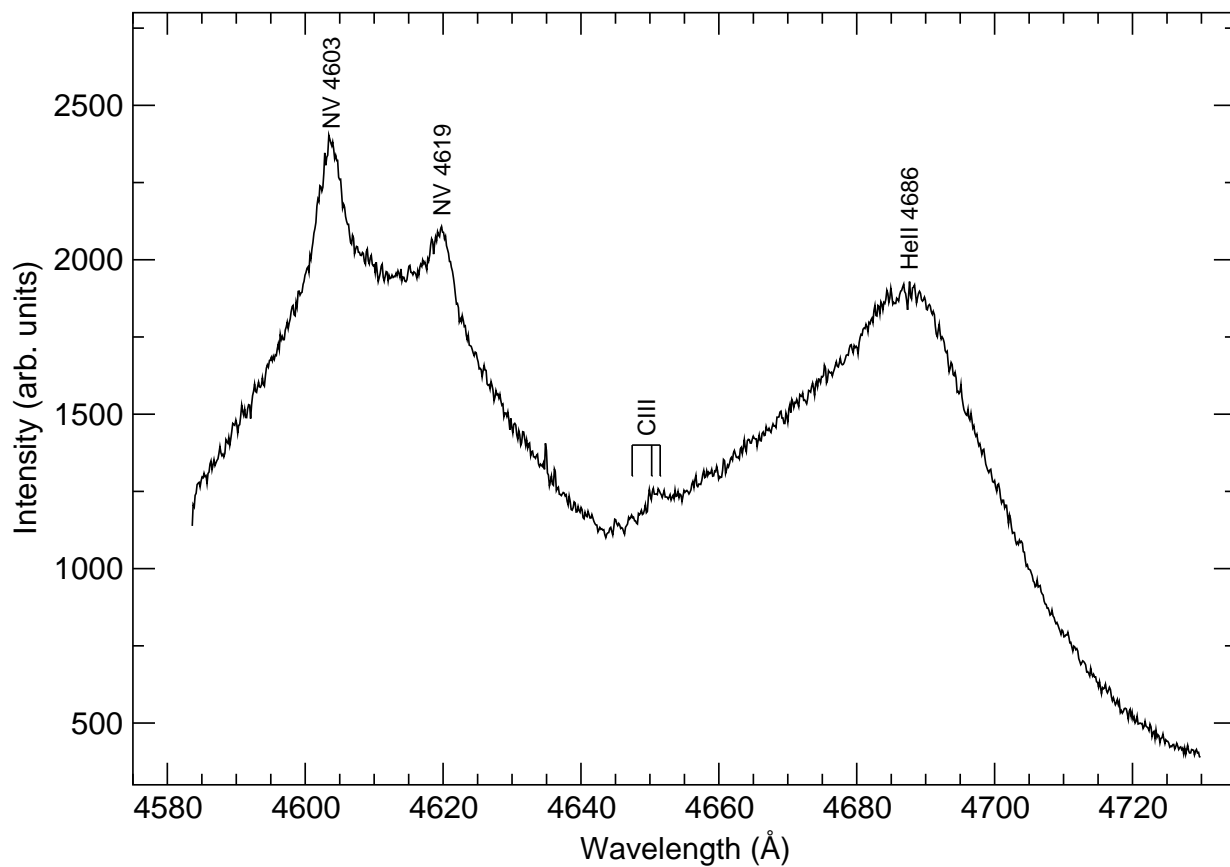


Fig. 3.— The average of the five high resolution spectra obtained on 1999 April 1, centered at 4650 Å. FWHM resolution is 0.23Å.

3.3. Continuum fluorescence vs. recombination

One noteworthy characteristic of the spectrum of this star is that the line widths of the N V lines at 4945Å and at 4603/19Å are very distinct. While the 4945Å line has FWHM $\sim 455 \text{ km s}^{-1}$, the 4603/19Å lines have a narrow and a strong broad component of width similar to that of He II 4686Å, that is, FWHM $\sim 2\,000 \text{ km s}^{-1}$. N V is, therefore, emitted in two different regions, with distinct kinematics. What does this mean in terms of physical interpretation?

The first point to notice is that the 4945Å line is a blend of a set of numerous recombination lines from the (6 – 7) transitions and also from the (8 – 11) transitions. The doublet 4603/19Å (transition $3s^2S - 3p^2P^0$) is formed by recombination from the cascading down process and also from the UV continuum fluorescence. The O VI 3811/34Å lines have similar structure.

The recombination emission depends on the square of the density while the continuum fluorescence lines have a linear dependence with density. If one assumes a wind that is optically thin for the exciting photons responsible for the fluorescence process and a velocity field given by

$$v(r) = v^* \left(1 - \frac{r^*}{r}\right)^\beta \quad (1)$$

where v^* is the terminal velocity of the wind, r^* is the radius of the star and β is a measure of the rate of acceleration (Castor et al. 1975), then the ratio of emissivity due to fluorescence (E_{fl}) and to recombination (E_{rec}) is

$$\frac{E_{fl}}{E_{rec}} \propto \left(1 - \frac{r^*}{r}\right)^\beta \quad (2)$$

This shows that the ratio E_{fl}/E_{rec} increases with radius to its maximum at $v = v^*$. The narrower recombination lines suggest that they are preferentially emitted in the inner part of the wind where density is higher and velocity is smaller. The continuum fluorescence lines are preferentially produced at higher velocities in the wind – similar to the ones seen in the He II emission.

There may be a hint about the nature of the N V 4603Å line variability in the line profile calculated by CSH95. In their Figure 6, the line profiles

from the two models considered are quite distinct. The two models have different effective temperatures and mass losses. The recombination lines are more sensitive to density and, therefore, to mass loss.

What we see in our data is that the recombination lines are less variable than the continuum fluorescence lines. The N V 4945Å recombination blend, for example, does not seem to vary as its TVS shows a velocity displacement pattern and not a lpv type profile. The continuum fluorescence lines are very sensitive to the central source effective temperature. A variable central source temperature is, therefore, the likely explanation for the N V 4603/19Å variability. This variability in temperature could be originated either in the stellar atmosphere or, more likely, in the optically thick wind with variable optical thickness. A variable optical depth in the wind could, in principle explain, at the same time, the high variability in the N V lines, the photometric variability and the fact that the star becomes bluer when fainter (Vee02a). CSH95 have calculated detailed models for the emission line profiles. In their figure 6 they show that the two models with effective temperatures of $T_{eff} = 80\,000 \text{ K}$ and $T_{eff} = 89\,000 \text{ K}$ both describe reasonably well the line N V 4945Å but the lines N V 4603/19Å are only adjusted well if the temperature is about $T_{eff} = 89\,000 \text{ K}$. This again argues in the sense that the intensity of these lines is much more sensitive to the stellar temperature than the N V 4945Å line.

We see significant evidence of variability in the degree of ionization. For instance, although we can not identify the N IV multiplet near 7123Å in the FEROS (2002) spectrum, in our spectrum taken in the 3400–3900Å region (1996) there is a strong emission of the N IV 3479Å multiplet. These two multiplets arise in the recombination cascading and correspond to successive transitions; being correlated, they should be both present or absent. An explanation for this apparent discrepancy may be that the star was at a higher degree of ionization in January 2002, when compared to June 1996 (see also a discussion about the variability of the N IV line in Vee02a).

The degree of ionization of a stellar wind is related to the ionization parameter (the density of ionizing photons divided by the electron density). The correlation between the N V 4603/19Å inten-

sity and the appearance of the C III line in Figure 3 (when compared to Figure 1) seems to point toward opposite directions. While a stronger emission of the N V lines in Figure 3 suggest a higher temperature, the presence of the low ionization species C III can only be reconciled if a high wind density is also assumed.

4. The 0.3319 d period

Radial velocity curves were constructed using N V 4603Å (spectra with 0.65Å and 0.23Å spectral resolution), N V 4945Å, He II 4686Å and O VI 3811Å (0.65Å resolution) emission lines measured at the Coudé spectrograph. N V 4945Å, N V 4603Å and O VI 3811Å from the FEROS spectra (0.1Å resolution) were also used. The determination of the radial velocity from the N V lines was made by fitting a Gaussian profile to the peak of the lines. In the particular case of the N V 4603Å we adjusted a Gaussian using the profile above 80 % of its height, given the proximity of the line at 4619Å and also because of the broad (fluorescence) component that may have a somewhat distinct kinematics. The radial velocity of the He II emission line was measured from the flux weighted centroid of the line.

The O VI 3811Å and the O VI 3834Å lines are very close to each other. Therefore the determination of their central wavelength was performed by deblending using two Gaussian components. All radial velocities were corrected to heliocentric velocity system and are given in Tables 5a and 5b.

The various lines in consideration here show distinct systemic velocities (see Table 6). This is so because of blending and self-absorption (in the case of He II). All lines have, in fact blending problems. N V 4603/19Å are blended with each other and also with He II 4686Å. The broad and variable component leaves the situation even worse. In the case of the O VI lines, the situation is similar but somewhat better as it is not blended with any other strong line. It seems that the most reliable radial velocity measurements come from N V 4945Å. This is, in fact, a blend of a forest of N V 6–7 (and also 8–11) transitions that happen to have similar wavelength. Since all are recombination lines and are emitted in the densest part of the wind, it seems to be a good indicator of the stellar kinematics. For this reason we subtracted from

each radial velocity measurement of N V 4603Å, the systematic difference between the average velocity of this line and that of N V 4945Å. This difference is 46 km s⁻¹. We also assigned different weights to spectra with distinct resolution: weight 2 to spectra with resolution 0.65Å and weight 3 to spectra with resolution 0.23Å and 0.10Å.

As found by Marchenko et al. (1998b), our data also show that DI Cru presents photometric variations with time-scales of months. The total amplitude of variations we observed is of about 0.45 mag. This seasonal type of variation is unique among WR stars. We also found that the photometric characteristics such as flickering activity and night to night light curve shape depend strongly on the level of the overall brightness. For this reason we separated the data in three groups, depending on the intensity. We will call these groups as minimum, intermediate and maximum brightness levels and will, as a first approach, analyze them separately in terms of periodicity searching routines. The minimum brightness level was arbitrarily defined by photometric measurements with $\Delta\text{mag}(v-c1) > -0.65$, where $\Delta\text{mag}(v-c1)$ is the difference in magnitudes between the variable star (DI Cru) and the comparison star c1 ($V=11.79$, $\alpha(\text{J2000})=12:05:24.5$, $\delta(\text{J2000})=-62:01:43.6$), in the V band. In the intermediate state $-0.85 > \Delta\text{mag}(v-c1) > -1.00$, and in the maximum state $-0.95 > \Delta\text{mag}(v-c1) > -1.10$.

We initially applied the Lomb-Scargle algorithm to search for periodicities in the radial velocity and intermediate level photometric data. The resultant periodograms are displayed in Figure 4, and show a main signal with $P = 0.3319$ d (3.013 cycles d⁻¹). An one day alias of 0.25 d (4.0 cycles d⁻¹) is also strong but less significant in the radial velocity data. The one month aliases of 0.324 and 0.340 d (3.09 and 2.94 cycles d⁻¹) are also quite strong and can not be discarded on the basis of these periodograms only. The high brightness level photometric data will be analyzed in Section 5.

The photometric ephemeris is:

$$T_{min}(HJD) = 2\,450\,917.297(\pm 20) + 0.3319(\pm 7) \times E \quad (3)$$

where T_{min} is the minimum of the intermediate level light curve (see Figure 7).

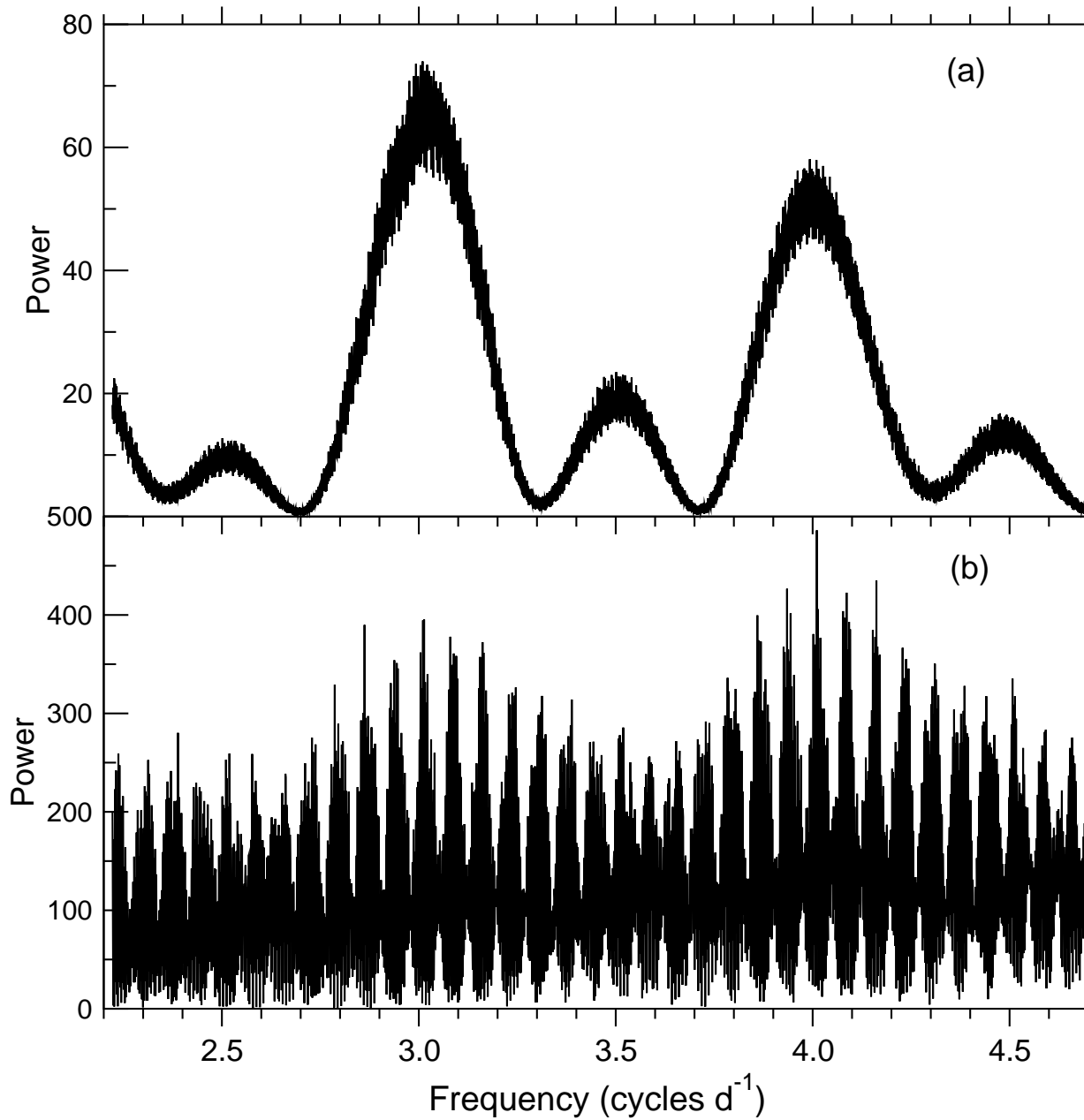


Fig. 4.— Lomb-Scargle periodograms of the radial velocity (a) and intermediate brightness level photometric (b) data.

The radial velocity curve is consistent with this period and the time of crossing from positive to negative values when compared to γ is $T_0(HJD) = 2\,450\,917.232(\pm 20)$. Figure 5 shows the radial velocity curve of the N V lines folded with the 0.3319 d period. The best fit sine-wave is also shown and yields the values of $\gamma = -69(\pm 2)$ km s⁻¹ for the systemic velocity and $K = 58(\pm 2)$ km s⁻¹ for the radial velocity semi-amplitude. We used the same values for the period and T_0 to plot the radial velocity curve of the He II emission line. As can be seen in Figure 6, it presents a significant phase lag (0.2 in phase) when compared to N V. This confirms the stratified nature of the wind as already shown by Vee02b.

One should notice the strong difference between our values for K and γ and those measured by Niemela et al. (1995). These authors found that the amplitudes of the radial velocity curves of the N V 4603/19Å and the He II 4686Å lines were, respectively, 320 km s⁻¹ and 173 km s⁻¹, while the systemic velocity determined from these same lines were also quite discrepant, namely +4 km s⁻¹ and +204 km s⁻¹. Similar differences between distinct lines have also been reported by Vee02b. This is, perhaps, not surprising as these lines are so badly blended. Spectral resolution also matters as the narrow component of N V can only be measured with some confidence for medium to high resolution spectra.

The average light curve of the intermediate brightness level with the period of 0.3319 day is shown in Figure 7. A double wave with two unequal minima is seen.

5. Multiple periodicities

The behavior of the radial velocity and intermediate level photometric data seems to be consistent with a single period phenomenon – the classical situation of a binary system. In the present analysis, however, the situation is clearly more complicated. This is well illustrated by the Lomb-Scargle periodograms for the photometric data obtained in the years 1997, 1998 and 1999 (Figure 8). The 1997 data, in which the star was at the intermediate brightness level, is consistent with a single period of $P_s = 0.3319$ d (3.013 cycles d⁻¹). In 1998 (intermediate/high levels) however, when radial velocity showed this same period, photometry

shows a distinct value of about 0.154 d (6.49 cycles d⁻¹).

The situation becomes even more complicated in 1999. In this season we have the best coverage and the star was more variable, being at its maximum photometric level. At least 3 periods are seen: 0.378, 0.254 and 0.183 d (2.65, 3.94 and 5.46 cycles d⁻¹), and none of them matches the previous values. An additional period of 0.583 d (1.72 cycles d⁻¹) seems to be present with weaker signal in the years of 1998 and 1999. Table 7 summarizes the principal periods found for this object.

The radial velocity measurements made by Marchenko et al. (2000) – Mar00 – allowed those authors to determine a period of 0.329 d. As these observations were made in 1999 March and we have spectroscopic observations from 1999 April/May, it is worthwhile to combine them and refine the analysis of the possible periods. To do this, we incorporated to our set of 1999 radial velocity data only the Mar00 data for the narrow N V 4945Å line, with weight 1 (our data kept weights as defined in Section 4). The first thing to notice in the resultant periodogram (Figure 9) is that, as expected, the strongest signal is in the range of frequencies of 3.01 – 3.05 cycles d⁻¹ (0.328 – 0.332 d). Surprisingly, there is a peak with about the same intensity at 3.74 cycles d⁻¹ (0.267 d). Other two peaks of weaker intensity appear at 4.29 and 3.60 cycles d⁻¹ (0.233 and 0.278 d). These periods are very close to the photometric periods found in the 1989 and 1991 data by Vee02a. The values of 3.74 and 3.60 cycles d⁻¹ (0.267 and 0.278 d) are also close to the oscillations seen in radial velocity data in 1989/1991 (Vee02b).

Combining these data with our measurements from 1998 we obtain the strongest peak at 3.014 cycles d⁻¹ (0.3318 d), which is about the same value (0.3319 d) determined in Section 4. In the same periodogram we also see a secondary peak at 3.55 cycles d⁻¹ (0.282 d). These secondary radial velocity periods are very important in terms of interpreting the nature of the star. First, multiple periods have been seen in photometry before but not in radial velocity. Second, the secondary periodogram peaks seen in the 1998/1999 radial velocity data recover the photometric periods seen in 1989/1991. This means that the star keeps its frequency memory and is not controlled by a sin-

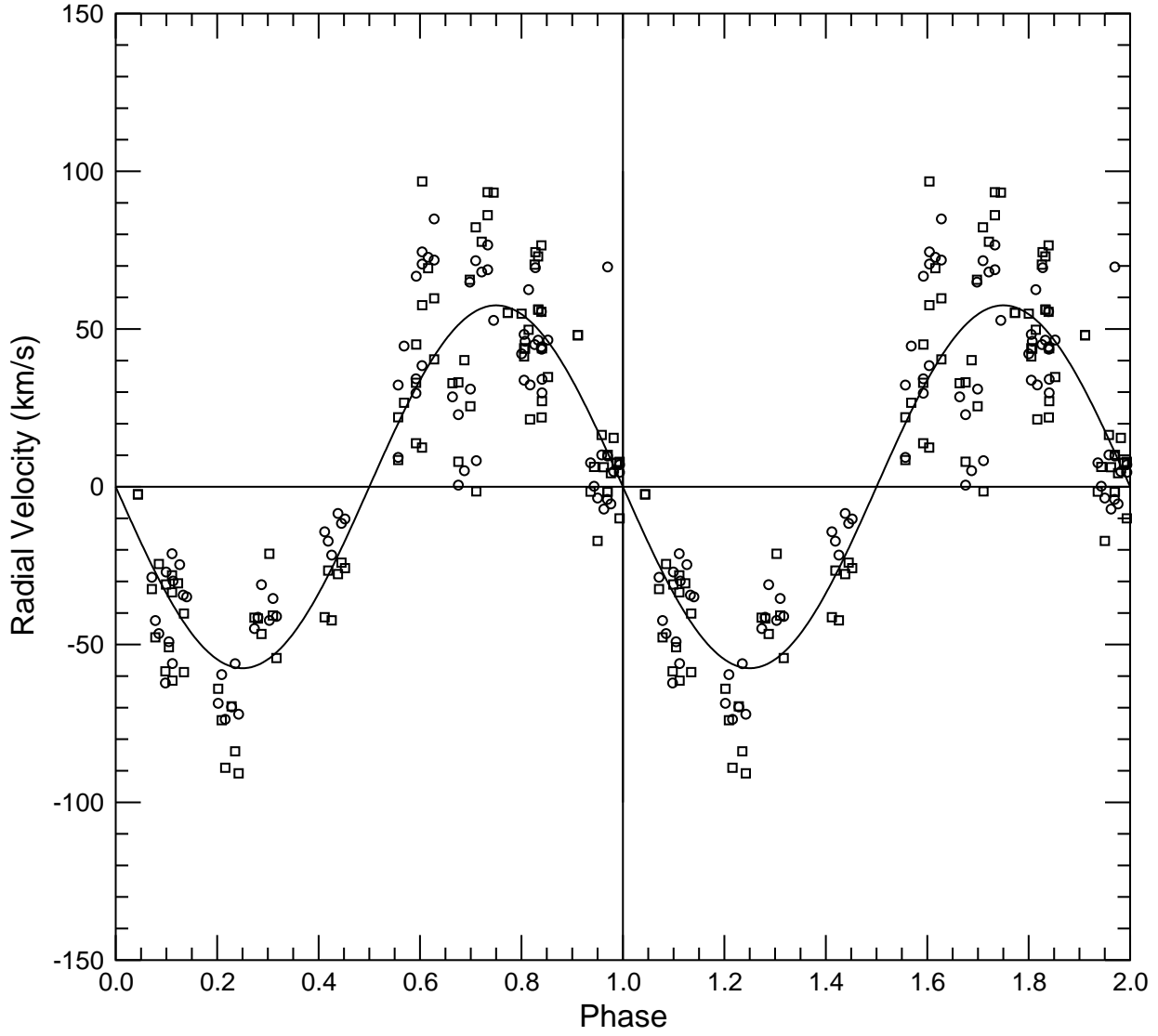


Fig. 5.— Radial velocity curve of the N V 4603Å (squares) and N V 4945Å (circles) emission lines folded with $P = 0.3319$ d and $T_0 = 2\,450\,917.232(\pm 20)$ HJD. The systemic velocity has been subtracted from the data.

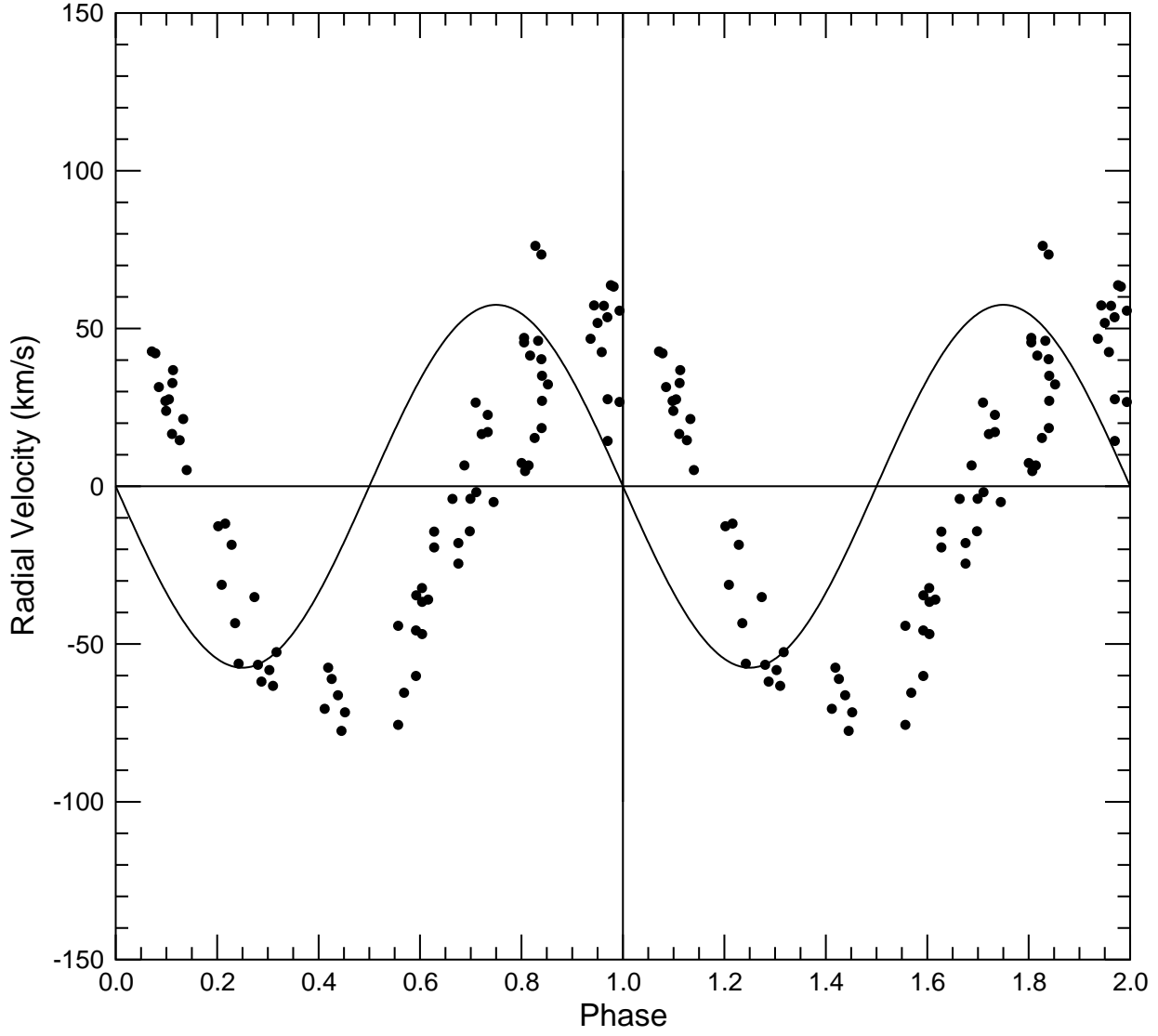


Fig. 6.— Radial velocity curve of the He II emission lines folded with $P = 0.3319$ d and $T_0 = 2\,450\,917.232(\pm 20)$ HJD. The line represents the sinusoid fit to the N V radial velocity data. The systemic velocity has been subtracted from the data.

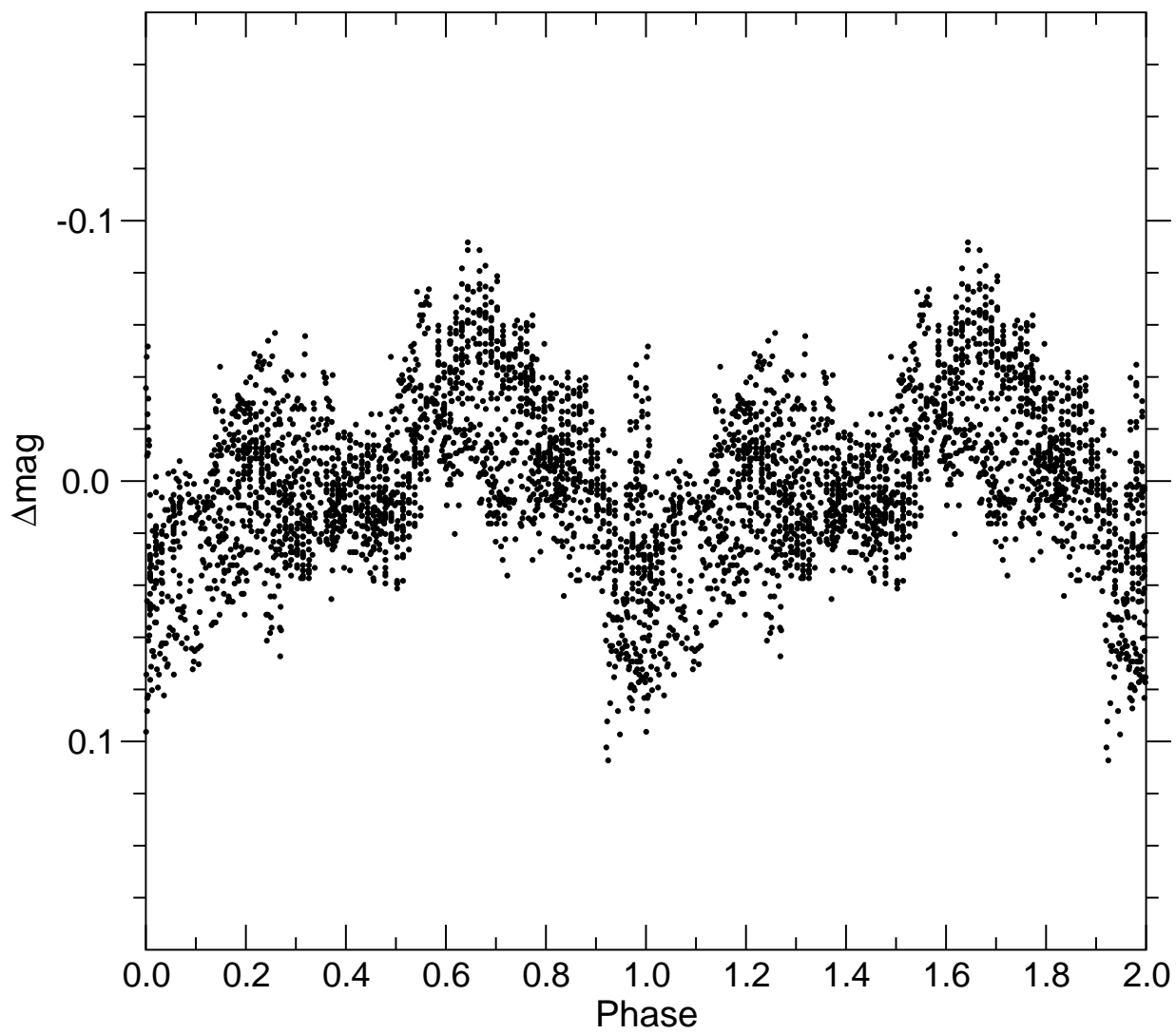


Fig. 7.— Intermediate brightness level average light curve of DI Cru, plotted in phase using the photometric ephemeris.

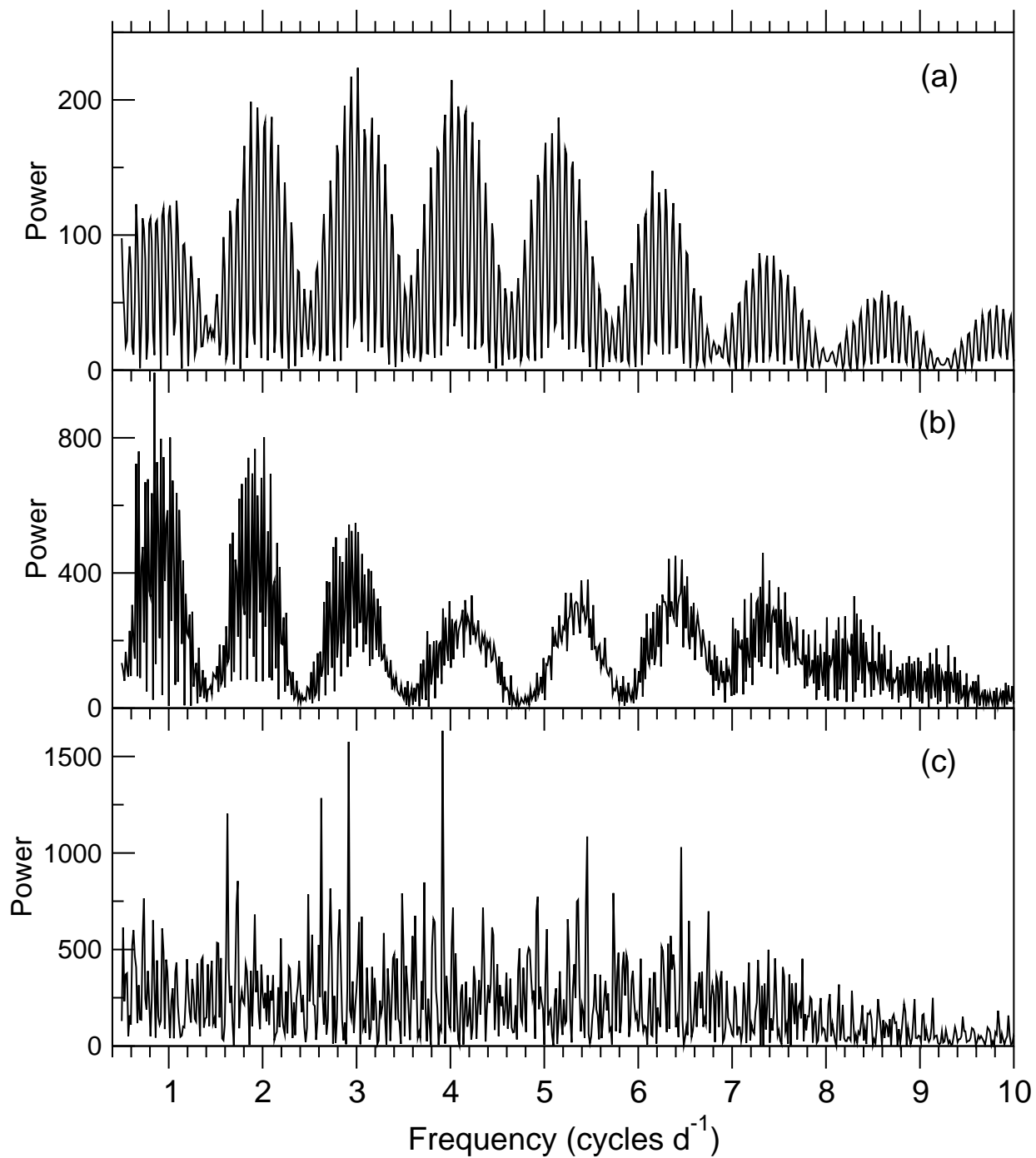


Fig. 8.— Lomb-Scargle periodograms for the photometric data obtained in the years 1997 (a), 1998 (b) and 1999 (c).

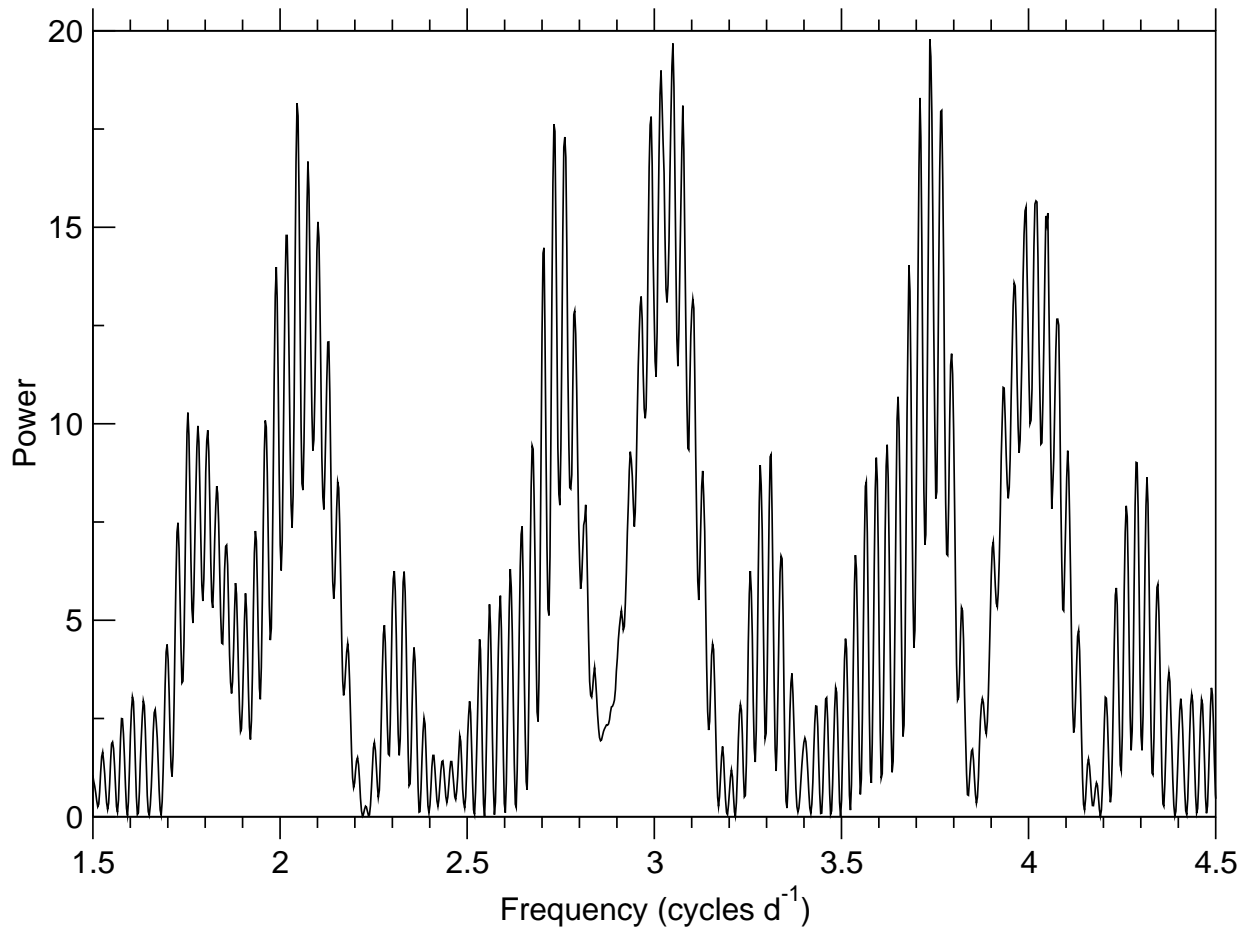


Fig. 9.— Lomb-Scargle periodogram for 1999 (LNA plus Mar00) radial velocities for the N V 4945Å lines.

gle clock with ever-growing period as suggested by Vee02b.

Mar00 and Vee02b observed a puzzling phenomenon in the radial velocity behavior of this star. Although periodicities with large amplitude are seen by both authors, from time-to-time they also observe a standstill so that the radial velocity does not vary at all along single nights. This unusual behavior seems to repeat with time-scales of 2 – 3 days.

Could this be caused by constructive/destructive interference between the distinct but simultaneously present multiple periods? A close inspection of the patterns shown in Figure 9 suggests that this might well be the case. As at least 4 periods seem to be present in the observations from 1999, one expects a rather complex pattern of interference. We expect, however, a main beat period as a result of the interference of the two main periods (0.329 d and 0.267 d). This gives a beat period of 1.43 d. But, given that this is about 3/2 of a day, the actual observations would have a recurrence time-scale of about 3.3 d. This is consistent with the observations of Mar00. This is a clear argument in favor of the explanation of the "standstill puzzle" as a consequence of interference between the periods that are present simultaneously.

6. Discussion

One aspect that must be considered carefully in radial velocity measurements is the resolution of the spectra, as well as the line under consideration. For example, Mar00 measured the radial velocity of the line blend of He II 4686Å + N V 4603/19Å. Given the high variability of the He II/N V line ratio, it is hard to tell what a radial velocity variation of such a blend would mean. A second point one must caution about is the mix of recombination and continuum fluorescence of the N V and O VI $3s\ 2S-3p\ 2P^0$ transition, as they are emitted in distinct regions within the wind. The broad component, formed in the high velocity and low density wind, probably due to fluorescence, may have a kinematics that is quite distinct from that of the narrow component, due to recombination. This conclusion one derives from Figure 1, considering that the broad component of N V has a kinematics similar to that of He II 4686Å. This last line must also be considered with care. Variable P

Cygni-type absorption introduces a radial velocity shift in the peak of the He II lines that may mask or substantially contaminate the radial velocity measurements. By comparing the average velocity of N V 4945Å to that of He II 4686Å, we conclude that this effect amounts to +130 km s⁻¹. From these considerations we believe that the most reliable measurements are those made from the peak of N V and O VI lines as they are the likely tracers of the stellar kinematics.

6.1. Is DI Cru a binary system?

Niemela et al. (1995) and Mar00, based on their radial velocity observations, have concluded that their spectroscopic period is likely to be the binary one. Although there is a difference between the two periods (0.311 d *vs.* 0.329 d) one has to consider that the period determined by Mar00 and by us is consistent with the idea that our main radial velocity period may, perhaps, be stable and represent the orbital one. The existence of secondary spectroscopic frequencies (3.74, 3.55, 4.29, 3.60 cycles d⁻¹, or 0.267, 0.282, 0.233, 0.278 d), however, shows how much care one has to take in analyzing this object.

The secondary spectroscopic periods found in 1998 and 1999 have recovered the photometric periods found in 1989/91. This strongly argues against the idea that the variability is controlled by a single clock with rapidly increasing clock-rate (Vee02a). On the contrary, it seems that distinct periods appear and reappear from time to time.

The existence of multiple spectroscopic periods also shows that the orbital period is not the only one. We conclude that we cannot rule out the hypothesis that DI Cru is a binary system; but its binary nature has not yet been proven. This could possible be done by demonstrating that the star shows long term coherence or by detecting the secondary star.

6.2. Non-radial oscillations

Vee02c have discussed in detail various possibilities to explain the observed characteristics of this star. Although not discarding the possibility of a binary system, they proposed non-radial oscillations as the likely cause of the observed photometric and spectroscopic variations. The main reason for this idea is that the photometric variations are

not strictly periodic and multiple frequencies seem to be present at a given epoch.

We show a summary of the photometric and spectroscopic (radial velocity) periods identified so far in Table 7. Most of the periods are either close to 3.0 – 3.7 cycles d^{-1} (0.270 – 0.333 d) or to 6.5 – 7.3 cycles d^{-1} (0.137 – 0.154 d). As pointed out by van Genderen et al. (1991), if the photometric data that show ~ 7 cycles d^{-1} (0.143 d) are folded using twice the single-wave period, the light curve appear ellipsoidal with unequal minima. Moreover, the radial velocity data obtained simultaneously with the photometry are in better agreement with the double-wave than with the single-wave period. Therefore we show, in parenthesis in Table 7, half the frequency in those cases. The distribution of periods that appear both in spectroscopy and photometry is now concentrated near 3.0 – 3.2 (0.313 – 0.333 d), 3.5 – 3.7 (0.270 – 0.286 d) and 4.3 cycles d^{-1} (0.233 d).

Vee02c have convincingly suggested that the photometric and radial velocity variations may be interpreted as non-radial oscillations. The presence of simultaneous multiple spectroscopic and photometric periods certainly requires such an interpretation, regardless of the binary nature of the star. The stratification of the wind, which is visible in the delay of the radial velocity curves (Figure 6) of He II and of the narrow component of N V ($\Delta\phi \sim 0.2$) is consistent with this interpretation.

The presence of multiple periods suggests that one may be dealing with multiple modes of oscillations, and we will not attempt to identify these modes because of the temporal distribution of our data.

It is interesting to compare WR 46 \equiv DI Cru with HD 45166, which has been studied in detail by Steiner and Oliveira (in prep.). We have shown that HD 45166 has an orbital period of 1.59 d and additional oscillations with periods between 2.4 hr and 15 hr that appear in distinct velocity ranges in the wind. These additional non-orbital periods are interpreted as non-radial oscillations of a helium main sequence star of mass $M_1 = 3.7M_\odot$. The wind is optically thin given that one can observe atmospheric absorption lines from the hot star and this marks a significant difference between the two stars under consideration (DI Cru and HD 45166). DI Cru has an optically thick wind. This differ-

ence likely results from the masses of the two stars which are extreme cases in the context of WNE objects. As a consequence, their luminosities and mass-loss rates are very distinct, implying totally different wind optical depths. It may be surprising that even so the stars present oscillations with similar periods. Within this context, we consider that DI Cru may be regarded as a luminous counterpart of the qWR star HD 45166.

6.3. Nature and classification

Is this star a WR or a CBSS? Here we list several arguments in favor of the former scenario: a) One indication that the star is not a CBSS is its luminosity ($\log L/L_\odot = 5.53$), as determined by CSH95, which is larger than the maximum Eddington luminosity for a white dwarf ($\log L/L_\odot = 4.81$). Other arguments in favor of a WR star are: b) evidence for non-radial oscillations with periods that seem to be compatible with the expected ones for helium burning stars; c) good agreement between the observed line profiles and the ones predicted by model calculations assuming that it is a population I WR star (CSH95) and d) mass-loss rate ($\log \dot{M}(M_\odot \text{ yr}^{-1}) = -5.2$) too large for the context of a CBSS. For a CBSS one expects a rate 100 times smaller.

The classification of DI Cru in van der Hucht (2001) is WN3 pec while SSM96 propose WN3b pec, where b stands for "broad". These authors considered that the star does not have hydrogen. We showed in Section ?? that the star does have hydrogen and in a measurable amount. Therefore we propose a classification of WN3b(h) pec in the SSM96 three dimensional classification system. This classification shows some features that are unusual in the context of WR stars: objects classified as WN3 as well as WNb do not usually show hydrogen. In addition, only three WN objects (WR 46, WR 48c and WR 109) in the catalog by van der Hucht (2001) show O VI emission.

Although we interpret the object as a binary system with an orbital period of 0.3319 d, its true binary nature has not yet been clearly demonstrated. We suggest that further medium to high resolution spectroscopy of the purely recombination (and narrow) line N V 4945Å may reveal long term coherence. Similarly, additional photometry, preferentially when at medium photometric level, is also encouraged.

7. Conclusions

The main conclusions of this paper are:

1. The optical spectrum of DI Cru is rich in strong emission lines of high ionization species, mostly dominated by He II, N V, N IV and O VI. Weak emission of C III and H β (and presumably of other Balmer lines) is also present. Emission lines have been compiled from the literature and identified from the ultraviolet to the infrared. In the UV, emission of O V and N IV is also observed together with very weak emission of C IV.
2. The N V/He II line ratio varies by a significant amount from night to night. The TVS analysis shows that the He II 4686Å line has P Cyg-like variable absorption while N V 4603/19Å lines have a strong and broad variable component. We propose that this variability is due to continuum fluorescence caused by excitation from a source (stellar atmosphere/optically thick wind) of variable temperature. We also show that the object has variable degree of ionization, probably caused by wind density variation.
3. From our 1998/1999 radial velocity measurements we derived a main period of 0.3319 d (3.013 cycles d⁻¹) with an amplitude of $K = 58 \text{ km s}^{-1}$. This period is similar to the one found by Mar00 from 1999 observations.
4. When at intermediate photometric level (1997), it is possible, also to derive a photometric period that is consistent with 0.3319 d. Its light curve shows two minima of unequal depths.
5. In the years of 1998/1999 multiple spectroscopic and photometric periods were present, including those reported for the years 1989/1991. This argues against the idea that the variability is controlled by a single clock with rapidly increasing clock rate (Vee02a).
6. Mar00 interpreted the period of 0.3319 d as the orbital one. We argue that the additional photometric and spectroscopic periods are associated to non-radial pulsations, as proposed by Vee02c.

7. We call attention to the similarity between the multiple oscillation periods present in the stars DI Cru and HD 45166, despite the extreme differences between these stars (in the context of WNE objects) due to their very distinct masses. Given the similarities, we suggest that it might be a luminous counterpart of the qWR star HD 45166.
8. Interference between the various periods explains the disappearance of radial velocity modulation, seen from time to time.
9. The most convincing evidence that the star is not a CBSS is its luminosity, as determined by CSH95, which is larger than the maximum Eddington luminosity for a white dwarf. Other arguments in favor of a WR star are: evidence for non-radial oscillation, good agreement in line profile fitting and large mass loss rate.
10. Although the object is a possible binary system with an orbital period of 0.3319 d, its true binary nature (long term coherence, detection of the secondary star) has not yet been demonstrated. We suggest that further medium to high resolution spectroscopy of the purely recombination (and narrow) line N V 4945Å may perhaps reveal long term coherence. Similarly, additional photometry, preferentially when at medium photometric level, is also encouraged.

We would like to thank the referee, Dr. D. Gies, for his constructive comments on a previous version of this paper. Thanks are due to A. Bruch, D. Cieslinski, E. Oliveira, G. Quast and C. A. Torres for obtaining photometry data and R. P. Campos for obtaining spectroscopy data. We are also grateful to F. J. Jablonski for kindly providing the DFT program used in the period search and to A. Kanaan for his detailed comments on the manuscript.

REFERENCES

- Castor, J. I., Abbott, D. C., & Klein, R. I. 1975, *ApJ*, 195, 157
- Cieslinski, D., Diaz, M. P., & Steiner, J. E. 1999, *AJ*, 117, 534

- Conti, P. S., & Vacca, W. D. 1990, *AJ*, 100, 431
- Crowther, P. A., Smith, L. J., & Hillier, D. J. 1995, *A&A*, 302, 457 – CSH95
- Diaz, M. P. 1999, *PASP*, 111, 76
- Diaz, M. P., & Steiner, J. E. 1995, *AJ*, 110, 1816
- Fullerton, A.W., Gies, D.R. & Bolton, C.T. 1996, *ApJ Supp*, 103, 475
- Hamann, W.-R., Koesterke, L., & Wessolowski, U. 1995, *A&AS*, 113, 459
- Herbig, G. H., Preston, G. W., Smak, J., & Paczynski, B. 1965, *ApJ*, 141, 617
- Kahabka, P., & van den Heuvel, E. P. J. 1997, *ARA&A*, 35, 69
- Kaufer, A., Stahl, S., Tubbesing, S., Norregard, P., Avila, G., François, P., Pasquini, L., & Pizzella, A. 1999 *The Messenger*, 95, 8
- Marchenko, S. V., Moffat, A. F. J., Eversberg, T., Morel, T., Hill, G. M., Tovmassian, G. H., & Seggewiss, W. 1998a, *MNRAS*, 294, 642
- Marchenko, S. V., Moffat, A. F. J., van der Hucht, K. A., Seggewiss, W., Schrijver, H., Stenholm, B., Lundstrom, I., Gunawan, D. Y. A. S., Sutantyo, W., van den Heuvel, E. P. J., De Cuyper, J. P., & Gómez, A. E. 1998b, *A&A*, 331, 1022
- Marchenko, S. V., Arias, J., Barbá, R., Balona, L., Moffat, A. F. J., Niemela, V. S., Shara, M. M., & Sterken, C. 2000, *AJ*, 120, 2101 – Mar00
- Monderen, P., De Loore, C. W. H., van der Hucht, K. A., & van Genderen, A. M. 1988, *A&A*, 195, 179
- Niemela, V. S., Barbá, R. H., & Shara, M. M. 1995, in *IAU Symp. 163, Wolf-Rayet Stars: Binaries, Colliding Winds, and Evolution*, ed. K.A. van der Hucht & P.M. Williams (Dordrecht: Kluwer), 245
- Pollock, A. M. T. 1987, *ApJ*, 320, 283
- Roberts, D. H., Lehar, J., & Dreher, J. W. 1987, *AJ*, 93, 968
- Scargle, J. D. 1982, *ApJ*, 263, 835
- Schmutz, W., Hamann, W.R., & Wessolowski, U. 1989, *A&A*, 210, 236
- Smith, L. F., Shara, M. M., & Moffat, A. F. J. 1996, *MNRAS*, 281, 163 – SSM96
- Steiner, J. E., & Diaz, M. P. 1998, *PASP*, 110, 276
- Steiner, J. E., Cieslinski, D., Jablonski, F. J., & Williams, R. E. 1999, *A&A*, 351, 1021
- Steiner, J. E. , & Oliveira, A. S., in preparation
- Stellingwerf, R. F. 1978, *ApJ*, 224, 953
- Tovmassian, H. M., Navarro, S. G., & Cardona, O. 1996, *AJ*, 111, 306
- Vacca, W. D., & Torres-Dodgen, A.V. 1990, *ApJS*, 73, 685
- van den Heuvel, E. P. J., Bhattacharya, D., Nomoto, K., & Rappaport, S. A. 1992, *A&A*, 262, 97
- van der Hucht, K. A. 2001, *New Astr. Rev.*, 45, 135
- van der Hucht, K. A., Hidayat, B., Admiranto, A. G., Supelli, K. R., & Doom, C. 1988, *A&A*, 199, 217
- van Genderen, A. M., et al. 1991, in *IAU Symp. 143, Wolf-Rayet Stars and Interrelations with Other Massive Stars in Galaxies*, ed. K.A. van der Hucht & B. Hidayat (Dordrecht: Kluwer), 129
- Veen, P. M., et al. 1995, in *IAU Symp. 163, Wolf-Rayet Stars: Binaries, Colliding Winds, and Evolution*, ed. K.A. van der Hucht & P.M. Williams (Dordrecht: Kluwer), 243
- Veen, P. M., van Genderen, A. M., & Jones, A. F. 1999, in *IAU Symp. 193, Wolf-Rayet phenomena in Massive Stars and Starburst Galaxies*, ed. K.A. van der Hucht, G. Koenigsberger & P.R.J. Eenens (ASP), 263
- Veen, P. M., & Wieringa, M. H. 2000, *A&A*, 363, 1026
- Veen, P. M., van Genderen, A. M., van der Hucht, K. A., Allen, W. H., Arentoft, T., & Sterken, C. 2002a, *A&A*, 385, 585 – Vee02a

Veen, P. M., van Genderen, A. M., Crowther, P. A., & van der Hucht, K. A. 2002b, *A&A*, 385, 600 – Vee02b

Veen, P. M., van Genderen, A. M., & van der Hucht, K. A. 2002c, *A&A*, 385, 619 – Vee02c

Vreux, J. M., Dennefeld, M., & Andrillat, Y. 1983, *A&AS*, 54, 437

Wessolowski, U., et al. 1995, in *IAU Symp. 163, Wolf-Rayet Stars: Binaries, Colliding Winds, and Evolution*, ed. K.A. van der Hucht & P.M. Williams (Dordrecht: Kluwer), 174

TABLE 1
 JOURNAL OF PHOTOMETRIC OBSERVATIONS OF DI CRU.

Date (UT)	Hours of Obs.	Number of Exps.	Exp. Time (s)	Telescope	Detector	Filter	Brightness Level
1996 Apr 04	3.1	174	10	B&C 60cm	CCD 048	V	Low
1996 Apr 05	5.0	309	10	B&C 60cm	CCD 048	V	Low
1996 Apr 06	6.2	407	10	B&C 60cm	CCD 048	V	Low
1996 Apr 29	7.4	1098	10	B&C 60cm	CCD 009	V	Intermediate
1996 May 25	3.0	295	10	Zeiss 60cm	CCD 009	V	Intermediate
1996 Jun 15	0.3	5	10	Zeiss 60cm	CCD 009	V	Intermediate
1997 Mar 25	4.1	199	40	Zeiss 60cm	CCD 009	V	Intermediate
1997 Mar 26	2.6	150	40	Zeiss 60cm	CCD 009	V	Intermediate
1997 Apr 08	4.1	216	40	Zeiss 60cm	CCD 009	V	Intermediate
1997 May 07	4.3	12373	1	Zeiss 60cm	CCD 301	clear	Unidentified ^a
1997 May 10	3.6	11026	1	Zeiss 60cm	CCD 301	clear	Unidentified ^a
1997 Jun 01	4.9	11224	1	B&C 60cm	CCD 301	clear	Unidentified ^a
1997 Jun 02	0.3	16	40	B&C 60cm	CCD 301	V	Intermediate
1997 Jul 10	2.9	7837	1	B&C 60cm	CCD 301	clear	Unidentified ^a
1998 Mar 03	2.0	68	40	Zeiss 60cm	CCD 048	V	Intermediate
1998 Mar 04	0.7	31	40	Zeiss 60cm	CCD 048	V	Intermediate
1998 Mar 05	4.1	140	40	Zeiss 60cm	CCD 048	V	Intermediate
1998 Mar 06	1.3	331	40	Zeiss 60cm	CCD 048	V	Intermediate
1998 Mar 16	0.2	11	20	B&C 60cm	CCD 301	V	Intermediate
1998 Mar 26	1.2	300	10	Zeiss 60cm	CCD 301	V	Unidentified ^a
1998 Apr 05	0.8	26	10	B&C 60cm	CCD 301	V	Unidentified ^a
1998 Apr 06	1.2	82	10	B&C 60cm	CCD 301	V	High
1998 Apr 08	1.1	66	15	B&C 60cm	CCD 301	V	High
1998 Apr 11	6.1	2135	10	B&C 60cm	CCD 301	V	High
1998 Apr 12	3.7	1281	10	B&C 60cm	CCD 301	V	High
1998 May 11	2.5	270	15	B&C 60cm	CCD 301	V	Unidentified ^a
1998 May 12	3.2	217	10	B&C 60cm	CCD 301	V	Unidentified ^a
1998 May 13	2.3	89	15	B&C 60cm	CCD 301	V	Unidentified ^a
1999 Mar 18	5.3	374	40	B&C 60cm	CCD 101	V	High
1999 Mar 19	9.1	800	30	B&C 60cm	CCD 101	V	High
1999 Mar 21	1.1	67	40	B&C 60cm	CCD 101	V	High
1999 Apr 02	7.8	1180	8	Zeiss 60cm	CCD 301	V	High
1999 Apr 04	1.9	375	8	Zeiss 60cm	CCD 301	V	High
1999 Apr 19	7.5	1400	10	Zeiss 60cm	CCD 101	V	Unidentified ^a
1999 Apr 22	0.7	150	10	Zeiss 60cm	CCD 101	V	Unidentified ^a
1999 Apr 23	3.8	2376	6	Zeiss 60cm	CCD 301	V	High
1999 Apr 29	3.3	494	10	Zeiss 60cm	CCD 301	V	High
1999 Apr 30	4.1	702	10	Zeiss 60cm	CCD 301	V	High
1999 May 02	6.2	1254	8	Zeiss 60cm	CCD 301	V	High
1999 May 03	6.9	1450	8	B&C 60cm	CCD 301	V	High
1999 Jun 22	1.1	217	10	Zeiss 60cm	CCD 301	V	High
1999 Jun 23	3.6	632	10	Zeiss 60cm	CCD 301	V	High
1999 Jun 24	3.0	580	9	B&C 60cm	CCD 301	V	High
1999 Jun 25	2.4	582	10	B&C 60cm	CCD 301	V	High

^aData obtained without the V filter or falling between the intermediate and high brightness levels.

TABLE 2
JOURNAL OF SPECTROSCOPIC OBSERVATIONS OF DI CRU.

Date (UT)	Instrument	Grating (1/mm)	Number of Exps.	Exp. Time (s)	FWHM Res. (Å)	Coverage (Å)	Brightness Level
1996 Jun 10	Cassegrain	1200	1	300	2	4175 to 5130	Intermediate ^a
1996 Jun 11	Cassegrain	1200	1	900	2	3300 to 3970	Intermediate ^a
1996 Jun 12	Cassegrain	1200	1	300	2	4175 to 5130	Intermediate ^a
1998 Apr 10	Coudé	600	21	180	0.7	4520 to 4960	High ^a
1998 Apr 11	Coudé	600	36	180	0.7	4520 to 4960	High ^b
1998 Apr 12	Coudé	600	24	180	0.7	4520 to 4960	High ^b
1999 Apr 01	Coudé	1800	5	1200	0.23	4580 to 4730	High ^a
1999 Apr 29	Coudé	600	2	600	0.7	3740 to 4040	High ^b
1999 Apr 30	Coudé	600	3	900	0.7	3740 to 4040	High ^b
1999 May 01	Coudé	600	11	1200	0.7	3740 to 4040	High ^a
1999 May 02	Coudé	600	13	1200	0.7	3740 to 4040	High ^b
1999 Jul 01	Coudé	600	6	300	0.7	8077 to 8523	Unidentified
2002 Jan 24	FEROS	...	4	900	0.1	3600 to 9000	Unidentified
2002 Jan 25	FEROS	...	2	900	0.1	3600 to 9000	Unidentified
2002 Jan 26	FEROS	...	3	900	0.1	3600 to 9000	Unidentified
2002 Jan 27	FEROS	...	2	900	0.1	3600 to 9000	Unidentified

^aEstimated from quasi simultaneous (1 day apart) photometry.

^bDetermined directly from simultaneous photometry.

TABLE 3
EMISSION LINE IDENTIFICATION AND PROPERTIES.

Species ID	λ_{obs} (Å)	RV(HC)(2002) (km s ⁻¹)	$-W_\lambda$ (2002) (Å)	FWHM (2002) (km s ⁻¹)	$-W_\lambda$ (96/98/99) (Å)	FWHM (96/98/99) (km s ⁻¹)
O VI (6-7)	3433.7	1.2	1135
N IV (3s-3p)	3474:	30:	3600:
N V (7-10)	3500:	2:	770:
N IV (1s-1p) ?	3660:	4:	5000:
O VI (3s-3p)	3810.5	-67	3.2	460	4	670
O VI (3s-3p)	3833.6	-50	1.0	370	2	705
He II (4-13)	4027.3	127	0.5	450
He II (4-12)	4103.2	239	1.0	660
He II (4-10)+H γ	4341.2	...	0.8	600
N V (7-9)	4518.3	-8	1.2	450
He II (4-9)	4542.9	87	1.1	490	1.4	640
N V (3s-3p)	4603.5/4619.9	-15/-5	49	2600	55	2140
He II (3-4)	4688.2	160	82	2460	85	2040
He II (4-8)+H β	4860.8	...	9	...	9	...
N V (6-7)	4944.6	2	7.9	395	5	440
O VI (7-8)	5289.8	-68	1.0	550
He II (4-7)	5413.9	...	19
N V (9-13)	5668:	...	0.6:	840
He II (5-15)	6407	29	0.5	425
N V (8-10)	6477.6	-48:	1.8	425
He II (4-6)+H α	6562.6	...	46
He II (5-13)	6682.6	-27	1.9	780
N V (9-12)	6744.7	-121	0.8	540
O VI (8-9)	7714:	67	1.4:	430

NOTE.—2002: FEROS data (0.1Å resolution); 1996: Cassegrain data (2Å resolution); 1998/1999: Coudé data (0.7Å resolution)

TABLE 4
THE CNO EMISSION LINE TABLE FOR DI CRU.

Transition	O		N		C	
	O V		N IV		C III	
IP (eV)	113.90		77.47		47.89	
Term	$\lambda(\text{\AA}) - W_\lambda(\text{\AA})$		$\lambda(\text{\AA}) - W_\lambda(\text{\AA})$		$\lambda(\text{\AA}) - W_\lambda(\text{\AA})$	
$2p\ ^1P^0 - 2p^2\ ^1D$	1371	y	1719	y	2297	bl
$3s\ ^3S - 3p\ ^3P^0$	2781	y	3479	-30:	4647	wk
	O VI		N V		C IV	
IP (eV)	138.12		97.89		64.49	
Term	$\lambda(\text{\AA}) - W_\lambda(\text{\AA})$		$\lambda(\text{\AA}) - W_\lambda(\text{\AA})$		$\lambda(\text{\AA}) - W_\lambda(\text{\AA})$	
$2s\ ^2S - 2p\ ^2P^0$	1032	...	1239	-11.6:	1548	wk
	1038	...	1243	...	1551	...
$3s\ ^2S - 3p\ ^2P^0$	3811	-3.2	4604	-39:	5801	< 0.15
	3834	-1.0	4620	-19:	5812	np
$4s\ ^2S - 4p\ ^2P^0$	9342	y	11331	...	14335	...
	9398	y	11374	...	14362	...
$5s\ ^2S - 5p\ ^2P^0$	18550	...	22572	...	28617	...
	19663:	...	22654	...	28675	...
(4-5)	1126	...	1620/55	bl	2530	...
(5-6)	2070	...	2981	y	4658	bl
(5-7)	1292	...	1860	...	2907	...
(6-7)	3435	-1.2	4945	-7.9	7726	tell
(6-8)	2083	...	2998	y	4685	bl
(7-8)	5291	-1.0	7618	y	11908	...
(7-9)	3143	...	4520	-1.2	7063	np
(8-9)	7715	-1.4	11110	...	17368	...
(7-10)	2431	...	3502	-2:	5471	np
(8-10)	4494	y?	6478	-1.8	10124	...
(9-10)	11033	np	15536	...	24278	...
(8-11)	3427	...	4943	y	7737	np
(9-11)	6202	bl	8927	y	13954	...
(10-11)	14590	...	21000	...	32808	...
(8-12)	2916	...	4198	bl	6560	...
(9-12)	4692	bl	6747	-0.8	10543	...
(10-12)	8284	...	11928	...	18635	...
(11-12)	19180	...	27593	...	43138	...

TABLE 4—*Continued*

Transition	O	N	C
(9-13)	3939: ...	5668 -0.6	8858 ...
(10-13)	6198: y?	8918: bl	13946 ...

NOTE.—Meaning of the codes: y = line present; bl = blended line; wk = weak line; np = line not present; tell = telluric line.

References. — IR: Schmutz et al. (1989); Vreux et al. (1983). Optical: Vee02a; CSH95; Vreux et al. (1983). UV: CSH95; Vacca and Torres-Dodgen (1990). Rest wavelengths and line identifications were obtained from: NIST Atomic Spectra Database (http://www.physics.nist.gov/cgi-bin/AtData/main_asd), Atomic Line List (<http://www.pa.uky.edu/~peter/atomic/>) and Atomic Molecular and Optical Database Systems (<http://amods.kaeri.re.kr/>).

TABLE 5A
 RADIAL VELOCITY: N V AND HE II DATA.

HJD (2,400,000+)	RV(km s ⁻¹) N V 4603Å	RV(km s ⁻¹) He II 4686Å	RV(km s ⁻¹) N V 4945Å
50245.4794	-59	...	-59
50247.3950	-19	...	-59
50914.4293	-13	-5	-62
50914.4316	1	27	-40
50914.4339	5	6	-27
50914.4401	-8	11	-38
50914.4424	-8	25	-42
50914.4447	-9	39	-33
50914.4783	44	57	-7
50914.4806	61	98	-0
50914.4829	56	88	-4
50914.4870	65	94	5
50914.4893	72	88	-3
50914.4916	72	66	-19
50914.5204	53	147	-2
50914.5227	55	144	-27
50914.5250	34	111	-16
50914.7737	24	36	-5
50914.7760	36	24	-1
50914.7783	75	34	3
50914.7824	48	35	1
50914.7847	19	52	13
50914.7870	38	57	0
50915.4619	12	67	-43
50915.4642	12	46	-71
50915.4665	-13	53	-49
50915.4704	19	78	-67
50915.4726	4	67	-41
50915.4749	-23	69	-63
50915.5071	23	117	-38
50915.5093	20	118	-23
50915.5116	0	112	-39
50915.5177	6	106	-42
50915.5201	23	98	-38
50915.5224	13	103	-25
50915.5583	-5	114	-62
50915.5606	-11	85	-2
50915.5629	-23	99	-62
50915.5669	-6	134	-67
50915.5692	-13	127	-67
50915.5715	-31	98	-65
50915.6054	-52	95	-99
50915.6077	-49	88	-93
50915.6100	-55	108	-102
50915.6144	-52	86	-96
50915.6167	-80	92	-106
50915.6190	-62	76	-107
50915.6679	-68	9	-103
50915.6731	-43	13	-114
50915.6754	-62	8	-107
50915.6777	-76	18	-113
50915.7092	-63	0	-86
50915.7115	-48	14	-89
50915.7138	-64	10	-93
50915.7179	-49	5	-80
50915.7202	-45	-7	-83
50915.7225	-47	-1	-82
50916.5019	34	78	-30
50916.5042	22	76	-26
50916.5065	28	78	-9
50916.5104	49	86	-27
50916.5127	52	117	-25
50916.5150	1	89	-28
50916.5470	-23	118	-64
50916.5493	-15	128	-72
50916.5516	-39	123	-75
50916.5557	-15	128	-79
50916.5580	-23	125	-76
50916.5603	-17	135	-77
50916.5918	-54	114	-100
50916.5941	-69	113	-114
50916.5964	-46	102	-118
50916.6007	-80	98	-134
50916.6030	-72	99	-121
50916.6053	-83	104	-128
50916.6353	-85	58	-140
50916.6376	-95	40	-131
50916.6399	-100	59	-145
50916.6440	-91	52	-142
50916.6463	-105	28	-128
50916.6486	-112	15	-144
51270.6301	34
51270.6501	35
51270.6760	27

TABLE 5A—*Continued*

HJD (2,400,000+)	RV(km s ⁻¹) N V 4603Å	RV(km s ⁻¹) He II 4686Å	RV(km s ⁻¹) N V 4945Å
51270.7015	-14
51270.7200	-24

TABLE 5B

RADIAL VELOCITY: O VI, N V AND HE II DATA.

HJD (2,400,000+)	RV(km s ⁻¹) O VI 3811Å	RV(km s ⁻¹) N V 4603Å	RV(km s ⁻¹) He II 4686Å	RV(km s ⁻¹) N V 4945Å
50246.3905	-83
51298.5841	-64
51298.5936	-85
51299.5865	-70
51299.6434	-105
51299.6842	-101
51300.4403	-116
51300.4590	-104
51300.4881	-69
51300.5041	-78
51300.5227	-25
51300.5437	-42
51300.5611	-6
51300.5797	-3
51300.5977	-6
51300.6395	-37
51300.6885	-140
51301.4251	-34
51301.4499	-8
51301.4660	-51
51301.4820	-41
51301.4982	-26
51301.5182	-75
51301.5371	-74
51301.5539	-93
51301.5706	-103
51301.5876	-102
51301.6232	-98
51301.6413	-123
51301.6578	-98
52299.7142	-125	-39	203	-103
52299.7264	-161	-82	187	-124
52299.7686	-122	-80	78	-117
52299.8048	-90	-71	41	-105
52300.7596	5	65	220	24
52300.7881	5	53	199	16
52301.7111	-33	-10	135	-51
52301.7234	-42	-5	182	-44
52301.7799	-27	8	224	-26
52302.7112	32	72	261	17
52302.7654	-6	18	280	-32

TABLE 6

RADIAL VELOCITY CURVE PARAMETERS.

Line	K (km s ⁻¹)	γ (km s ⁻¹)
O VI 3811Å	28(±9)	-76(±7)
N V 4603Å	59(±3)	-24(±2)
N V 4945Å	54(±3)	-70(±2)
He II4686Å	61(±2)	61(±2)

TABLE 7
PHOTOMETRIC AND RADIAL VELOCITY FREQUENCIES.

Year	Photometry ^a (cycles d ⁻¹)	Ref. ^b	Radial Velocity (cycles d ⁻¹)	Ref. ^b
1989	7.08 (3.54) ; 4.34	(1)	3.54	(5)
1990	7.06: (3.53:); 4.35:	(1)	...	
1991	7.34 (3.67) ; 3.59:	(1)	3.67	(5)
1993/1994	...		3.21	(2)
1995	3.7:	(1)	3.7:	(5)
1997	3.01	(3)	...	
1998	6.49 (3.24) ; 3.7:; 1.71:	(1,3)	3.01 ; 3.55	(3)
1999	2.65; 3.94 ; 5.46 (2.73); 1.72:	(3)	3.04 ; 3.74; 4.29; 3.60	(4, 3)

^aNumbers in parenthesis are double-wave frequencies (half the photometric frequency – see Vee02a); bold-face numbers are the dominant frequencies.

^bReferences: (1) Vee02a; (2) Niemela et al. (1995); (3) This paper; (4) Mar00; (5) Vee02b